

GDSW Preconditioners for the EMI Model in Cardiac Electrophysiology

Edoardo Centofanti^[0000-0001-6834-0982],
Ngoc Mai Monica Huynh^[0000-0003-3639-5844],
Luca F. Pavarino^[0000-0002-3014-4668],
Simone Scacchi^[0000-0001-6011-784X]

1 Introduction

Advances in numerical methods and high-performance computing have greatly enhanced our ability to simulate complex biological systems with increasing accuracy. In cardiac electrophysiology, the Extracellular–Membrane–Intracellular (EMI) model [11, 13, 14, 15] has emerged as a highly detailed framework for representing the intricate biophysical interactions at the cellular scale. Unlike homogenized approaches such as the Monodomain and Bidomain models [3, 4], the EMI model explicitly resolves individual myocytes, their membranes, and the surrounding extracellular space. This microscopic representation enables the investigation of fine-scale electrophysiological mechanisms, including arrhythmogenic behaviors and the effects of structural heterogeneities such as fibrosis and ischemia.

However, the computational burden associated with the EMI model is extremely high, due to the large number of degrees of freedom and the strong discontinuities at membrane interfaces [10, 15]. The development of efficient, scalable solvers is therefore essential to enable simulations of realistic tissue domains. Among parallel strategies, domain decomposition (DD) methods have shown remarkable effectiveness, particularly Balancing Domain Decomposition by Constraints (BDDC) preconditioners [7, 8], which have exhibited robust performance for two-dimensional EMI problems. DD methods are suitable for the solution of multiphysics and multi-compartments problems, since they rely on the idea of dividing the problem (or its domain) into smaller subproblems (subdomains). In the context of the EMI model, the correspondence between myocytes and subdomain comes naturally. In addition,

Edoardo Centofanti · Luca F. Pavarino
Department of Mathematics, University of Pavia, Via Ferrata 5, Pavia, Italy, e-mail:
edoardo.centofanti01@universitadipavia.it, luca.pavarino@unipv.it

Ngoc Mai Monica Huynh · Simone Scacchi
Department of Mathematics, University of Milan, Via Saldini 50, Milan, Italy, e-mail:
ngoc.huynh@unimi.it, simone.scacchi@unimi.it

Algebraic Multigrid (AMG) techniques have been successfully employed as preconditioners for the same model, demonstrating excellent scalability and efficiency, including implementations on GPU architectures [2].

In this work, we introduce and investigate the Generalized Dryja–Smith–Widlund (GDSW) preconditioner applied to the EMI model. A previous related work has been proposed in [8], where a theoretical analysis and extensive tests were performed in a two-dimensional scenario. We present numerical results on both two- and three-dimensional structured meshes.

2 Mathematical models

We introduce here the formulation of the *cell-by-cell (EMI) model* [15] adopted in this work, which closely follows the one presented in [8].

Let $\Omega \subset \mathbb{R}^3$ denote the cardiac tissue domain, composed of $N + 1$ subdomains representing N cells $\Omega_i, i = 1, \dots, N$, embedded in the extracellular space Ω_0 . The cells are connected through *gap junctions*, protein channels that enable the exchange of ionic species between adjacent cells, while *ionic channels* in the cellular membranes mediate ionic current flow between each cell and the extracellular environment.

The EMI model is described by the following system of PDEs, coupled with a stiff ODE system:

$$\begin{cases} -\nabla \cdot (\sigma_0 \nabla u_0) = I_{\text{app}} & \text{in } \Omega_0, \\ -\nabla \cdot (\sigma_i \nabla u_i) = 0 & \text{in } \Omega_i, \quad i = 1, \dots, N, \\ -n_i^\top \sigma_i \nabla u_i = C_m \frac{\partial v_{ij}}{\partial t} + F(v_{ij}, w) & \text{on } E_{ij} = \overline{\Omega}_i \cap \overline{\Omega}_j \subset \partial\Omega_i, \\ \frac{\partial w}{\partial t} - R(v_{ij}, w) = 0 & \text{on } E_{i0}, \quad i = 1, \dots, N, \end{cases} \quad (1)$$

where $v_{ij} = u_i - u_j$ denotes the potential jump across the interface E_{ij} between adjacent subdomains Ω_i and Ω_j , σ_i is the conductivity tensor in Ω_i , n_i is the outward unit normal to $\partial\Omega_i$, and C_m is the membrane capacitance per unit area. The term $F(v_{ij}, w)$ depends on the type of interface considered, and it models either the ionic current through the cellular membrane or the gap-junction current.

The last two equations in (1) define the *membrane model*, an ODE system describing ionic dynamics. The variable w collects the gating variables associated with ionic channel behavior, while $R(v_{ij}, w)$ is a (generally nonlinear) function describing their temporal evolution. In this work, we adopt the *Luo–Rudy–Ranjan* model [12] for the membrane dynamics, and we refer to [16] for the mathematical analysis of system (1). Since the convergence of the preconditioned solver depends on the spectral properties of the preconditioner operator, which are not affected by the ionic model, we do not expect substantial changes in convergence behavior when using more complex or stiffer ionic models.

To introduce the discretization strategy, we recall the weak formulation of system (1). Integrating by parts over Ω_i the first two equations of (1) and applying the

third one on the membrane yields, for each subdomain Ω_i , the problem of finding $u_i(\cdot) : (0, T) \rightarrow H^1(\Omega_i)$ such that

$$\int_{\Omega_i} \sigma_i \nabla u_i \cdot \nabla \phi_i \, dx + \sum_{E_{ij}} \int_{E_{ij}} \left(C_m \frac{\partial v_{ij}}{\partial t} + F(v_{ij}, w) \right) \phi_i \, ds = 0, \quad \forall \phi_i \in H^1(\Omega_i).$$

Summing over all $N + 1$ subdomains, the global weak formulation reads:

$$\sum_{i=0}^N \int_{\Omega_i} \sigma_i \nabla u_i \cdot \nabla \phi_i \, dx + \frac{1}{2} \sum_{i=0}^N \sum_{E_{ij}} \int_{E_{ij}} \left(C_m \frac{\partial \llbracket u \rrbracket_{ij}}{\partial t} + F(\llbracket u \rrbracket_{ij}, w) \right) \llbracket \phi \rrbracket_{ij} \, ds = 0,$$

where $\llbracket u \rrbracket_{ij} = u_i - u_j$ and $\llbracket \phi \rrbracket_{ij} = \phi_i - \phi_j$ denote the jumps due to the discontinuity of the electric potential and of the test function across the interface $E_{ij} \subset \partial\Omega_i$.

3 Numerical methods

Space and time discretization. We consider an implicit-explicit (IMEX) time scheme, where the diffusion term is treated implicitly and the reaction term explicitly. We subdivide the time interval $[0, T]$ into K intervals and, by defining the time step $\tau = t^{(k+1)} - t^{(k)}$, for $k = 0, \dots, K$, we derive the following scheme:

1. Given the transmembrane potential from the previous time step $\llbracket u^{(k)} \rrbracket$, solve the membrane model $w^{(k+1)} = w^{(k)} + \tau R(\llbracket u^{(k)} \rrbracket_{i0}, w^{(k)})$ for $i = 1, \dots, N$.
2. Given the newly computed gating variable $w^{(k+1)}$, solve and update the diffusion systems $d_i(u_i, \phi_i) = f_i(\phi_i)$ for $i = 0, \dots, N$ at time step $(k + 1)$, where $d_i(u_i, \phi_i) := \tau a_i(u_i, \phi_i) + p_i(u_i, \phi_i)$,

$$a_i(u_i, \phi_i) := \int_{\Omega_i} \sigma_i \nabla u_i \cdot \nabla \phi_i \, dx, \quad p_i(u_i, \phi_i) := \frac{1}{2} \sum_{\substack{j \in \mathcal{E}_i^0, \\ j \neq i}} \int_{E_{ij}} C_m \llbracket u \rrbracket_{ij} \llbracket \phi \rrbracket_{ij} \, ds,$$

$$f_i(\phi_i) := \frac{1}{2} \sum_{\substack{j \in \mathcal{E}_i^0, \\ j \neq i}} \int_{E_{ij}} \left(C_m \llbracket u \rrbracket_{ij} \llbracket \phi \rrbracket_{ij} - \tau F(\llbracket u \rrbracket_{ij}, w^{(k+1)}) \llbracket \phi \rrbracket_{ij} \right) \, ds.$$

For the space discretization, we employ two- and three-dimensional Q1 finite elements. Let $V_i(\overline{\Omega}_i)$ be the regular finite element space of piecewise continuous linear functions in $\overline{\Omega}_i$ and define $V(\Omega) = V_0(\overline{\Omega}_0) \times \dots \times V_N(\overline{\Omega}_N)$ as the global finite element space. In this scenario the general problem reads as follows: find $u = \{u_i\}_{i=0}^N \in V(\Omega)$ such that

$$d_h(u, \phi) = f(\phi), \quad \forall \phi = \{\phi_i\}_{i=0}^N \in V(\Omega), \quad (2)$$

where $d_h(u, \phi) := \sum_{i=0}^N d_i(u_i, \phi_i)$ and $f(\phi) := \sum_{i=0}^N f_i(\phi_i)$. Thus, the problem (2) can be written in matrix form as

$$\mathcal{K}u = \mathbf{f}, \quad \text{with } \mathcal{K} = \sum_{i=0}^N \mathcal{K}_i, \quad \mathcal{K}_i = \tau A_i + M_i \quad (3)$$

where A_i and M_i are the local stiffness and mass matrices, respectively. We notice that the mass matrix is built only on the common interfaces E_{ij} between two subdomains Ω_i and Ω_j . The matrices \mathcal{K}_i , A_i , and M_i are all square, with dimensions corresponding to the number of degrees of freedom (dofs) [8, 9].

The GDSW preconditioner. We consider an overlapping Schwarz preconditioner of *Generalized Dryja–Smith–Widlund* (GDSW) type [5] for the problem (1), where the solution $u = \{u_i\}_{i=0}^N$ is discontinuous across subdomains Ω_i . The method combines a global coarse correction with local overlapping solves. The computational domain $\Omega = \bigcup_{i=0}^N \Omega_i$ is decomposed into non-overlapping subdomains, each extended to an overlapping region $\Omega'_i = \Omega_i \cup \Gamma_{i,\delta}$ of minimal thickness $\delta = h$. The local finite element spaces are $V_i = V^h(\Omega_i)$ and $V'_i = \{v \in V : v = 0 \text{ in } \Omega \setminus \Omega'_i\}$.

Coarse space. The coarse space V_0^C is spanned by *vertex* and *edge* basis functions, discrete harmonic inside each Ω_i . Denoting by ϑ_k^l the basis function associated to the vertex \mathcal{V}^l that has support in Ω_k , namely $\vartheta^l(x) = \{\vartheta_k^l(x)\}_{k \in \mathcal{V}_l^0}$, the coarse component $u_0 \in V_0^C$ can be written as

$$u_0 = \sum_{\mathcal{V}^l} \sum_{k \in \mathcal{V}_l^0} u_k(\mathcal{V}^l) \vartheta_k^l(x) + \sum_{E_{ij}} \bar{u}_{E_{ij}} \vartheta_{E_{ij}}(x), \quad (4)$$

where \mathcal{V}_l^0 is the set of indices k of the subdomain Ω_k that share the vertex \mathcal{V}^l , $\bar{u}_{E_{ij}}$ is the average of u on interface edge E_{ij} and $\vartheta_{E_{ij}}$ are edge functions, unique for each edge E_{ij} , equal to 1 on the edge E_{ij} and extended harmonically elsewhere. The corresponding coarse projection P_0 is thus defined by $d(P_0 u, v) = d(u, v)$, $\forall v \in V_0^C$. The EMI discrete harmonic extension is thus obtained by solving a local EMI Dirichlet problem. For a direct comparison with EMI-BDDC solver, refer to [8] and in particular to Section 5.2.1.

Local spaces and Preconditioned operator. Denoting the local non-overlapping finite element space by $V_i = V^h(\Omega_i)$, while the product space can be trivially written as $V = V_0 \times \dots \times V_N$, we then define the local space as $V'_i = \{v \in V : v = 0 \text{ in } \Omega \setminus \Omega'_i\}$, or, equivalently as $V'_i = V_i \times \{\phi_j : \phi_j \neq 0 \text{ on } \partial\Omega_i, \phi_j \notin V_i\}$. Since $V'_i \subset V$, any function $u'_i \in V'_i$ can be written as $u'_i = \{u'_{i,j}\}_{j=0}^N$. Let $\chi_i, i = 0, \dots, N$ be partition of unity as defined in [5]. Any function $u \in V$ can be written as

$$u = u_0 + \sum_{i=0}^N u'_i, \quad u_0 \in V_0^C, \quad u'_i \in V'_i, \text{ for } i = 1, \dots, N.$$

where $u_0 \in V_0^C$ has been defined in (4) and $u'_i \in V'_i$ are given by $u'_i = I^h(\chi_i(u - u_0)) \in V'_i \subset V$, where I^h interpolates into the product space $V^h(\Omega)$. The projection-like operators P_i onto the local space V'_i are defined as $P_i = I_i \tilde{P}_i$, where

$$d_h(P_i u, v_i) = d_h(u, v_i), \quad \forall v_i \in V'_i.$$

The GDSW preconditioned operator is then defined as $P_{ad} = P_0 + \sum_{i=1}^N P_i$. For further theoretical results, including quasi-optimality results in two-dimensions, the interested reader can refer to [9].

4 Numerical results

The 2D numerical tests were performed with our MATLAB implementations, while the 3D numerical tests were performed with our *in-house* Fortran90 code, based on the PETSc library. Regarding the local problem solves, we used the PETSc LU implementation to compute the discrete harmonic extension in the construction of the coarse solver, and the PETSc ILU implementation for inexact local solves in the one level part of the GDSW preconditioner. [1]. In all the following tests, the linear system at each time step is solved using the conjugate gradient (CG) method with a 10^{-8} reduction of the l^2 norm of the relative residual as a stopping criterion. The considered 3D geometry is depicted in Figure 1. We consider a three-dimensional slab of cells represented as a group of regular, elongated parallelepipeds connected through smaller blocks (here representing gap junctions); each parallelepiped is constructed in order to keep the ratio of 6:1, which is more likely the proportion of a healthy myocyte. The whole slab then is immersed in the extracellular space. The corresponding 2D geometry can be interpreted as a planar cross-section of this 3D configuration, taken along a plane intersecting the gap junctions. In all tests, the membrane capacitance is $C_m = 1 \mu F/cm^2$, the extracellular conductivity is $\sigma_0 = 2e - 3 \Omega^{-1}cm^{-1}$ and the intracellular conductivity is $\sigma_i = 2e - 3 \Omega^{-1}cm^{-1}$, for $i = 1, \dots, N$. We include optimality tests for the two-dimensional scenario, and both strong and weak scaling tests for the three-dimensional one. We point out that, in all the following tests regarding the GDSW implementation, the computational cost for the coarse solver is about the 30-40% of the cost of the local solvers.

2D optimality tests. We first test the quasi-optimality of EMI-GDSW. The number of cells (subdomains) is fixed to $N = 4 \times 4$, while the mesh size h is decreasing (i.e. the ratio H/h is increased). In these tests, the EMI-GDSW coarse solver has dimensions 112×112 and 1844 nonzero entries. Table 1 shows the better performance of the EMI-GDSW solver against Additive Schwarz (AS) preconditioner for the CG method. The polylogarithmic growth of the EMI-GDSW condition number is not easily detectable for this range of H/h , but the growth appears to be clearly sublinear. In order to detect the asymptotic behavior of the EMI-GDSW condition number, higher values of H/h should be explored as in [6], but this was currently beyond our actual computational capability using a Matlab implementation on a workstation.

3D weak scaling test. The weak scaling performance of the proposed EMI-GDSW solver was evaluated on the CINECA G100 cluster, equipped with Intel Xeon Platinum processors running at 2.4 GHz, with 48 cores per node. All tests were performed using PETSc 3.20.2, with solver tolerances set to `-ksp_rtol 1e-6` and `-ksp_atol 1e-8`. In this experiment, we kept the local problem size fixed and increased the number of processors. Each group of 4 CPUs handles approximately a

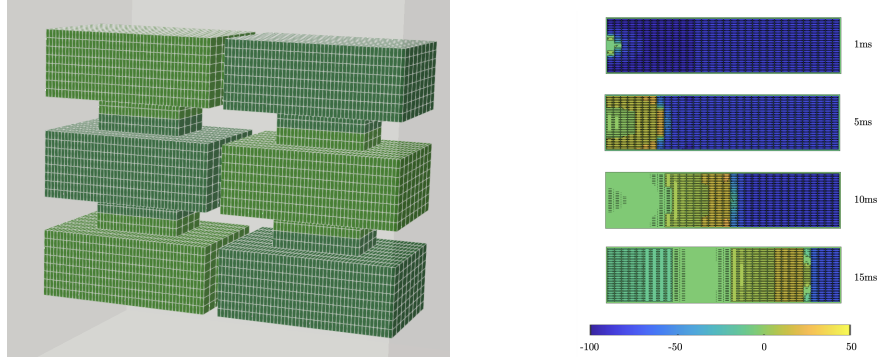


Fig. 1 Left: three-dimensional geometry with $2 \times 3 \times 1$ cells (each with # elements) surrounded by the extracellular liquid. The interconnection between cells are gap junctions (smaller blocks). Right: top view snapshots of the potential u_i up to $t = 15$ ms for a $32 \times 32 \times 1$ cell slab. The color map illustrates the spatial distribution of the intracellular potential (in mV).

H/h	N_{dof}	EMI-GDSW		AS	
		k_2	it	k_2	it
12	984	54.3	34	313.6	43
18	1936	73.3	39	473.7	51
24	3200	90.1	43	632.4	58
30	4776	103.7	46	791.5	63
36	6664	118.1	49	945.1	68
42	8864	130.8	50	1.10e+03	73
48	11376	143.8	52	1.26e+03	77
54	14200	148.3	54	1.41e+03	80
60	17336	163.2	56	1.57e+03	83

Table 1 2D numerical tests. Optimality tests. Condition number (k_2) and linear iterations (it) at final time $t = 5$ ms for EMI-GDSW (left) and AS (right).

tissue slab of $4 \times 2 \times 1$ cells, yielding approximately 300k local degrees of freedom (DOFs). Each cell was discretized using $48 \times 8 \times 8$ trilinear (Q1) finite elements. The total simulated time was 2 ms, with a time step $\tau = 0.01$ ms, and electrical activation was initiated by a 1 ms stimulus applied to the left face of each slab domain.

Table 2 reports the weak scaling results obtained for the EMI-AMG solvers (GAMG, HYPRE) and the proposed EMI-GDSW solver. The number of CG iterations and the average CPU time per time step are shown as functions of the number of cores and total DOFs. The EMI-GDSW preconditioner maintains nearly constant iteration counts as the problem size grows, confirming its good scalability. In contrast, AMG-based solvers exhibit a progressive increase in iteration counts, particularly for larger core counts. The execution times per step remain competitive for EMI-GDSW across all configurations, with significantly lower costs than AMG-based solvers for the largest problems.

# CPU	cells	# DOFs	GAMG		HYPRE		EMI-GDSW	
			it	time	it	time	it	time
4	$4 \times 2 \times 1$	281,803	29.7	9.82	14.9	9.56	7.16	5.34
8	$4 \times 4 \times 1$	453,301	31.3	8.99	15.8	8.49	9.89	5.42
16	$8 \times 4 \times 1$	874,777	35.8	14.68	19.9	12.45	14.47	9.96
32	$8 \times 8 \times 1$	1,537,325	37.4	18.32	22.8	13.69	16.82	9.82
64	$16 \times 8 \times 1$	3,019,381	41.2	17.83	29.5	21.22	16.55	11.27
128	$16 \times 16 \times 1$	5,622,685	43.2	20.30	39.9	25.47	18.23	7.98
256	$32 \times 16 \times 1$	11,143,213	57.4	35.93	55.0	40.28	18.09	8.98
512	$32 \times 32 \times 1$	21,462,653	64.2	40.26	68.5	89.48	19.19	13.10

Table 2 3D numerical tests. Weak scaling of EMI-AMG (GAMG, HYPRE) and EMI-GDSW solvers. Average CG iterations (it) and average CPU time per time step (in seconds) as a function of the number of cores and DOFs.

5 Conclusions

In this work, we investigated the GDSW preconditioner applied to the EMI model in both two and three dimensions. Our results demonstrate the scalability and efficiency of the proposed EMI-GDSW solver, establishing it as a promising tool for large-scale simulations of cardiac electrophysiology at the microscopic level. In future works, we plan to extend the construction of the GDSW preconditioner to unstructured finite element meshes, where we expect similar scalability properties, possibly with a moderate increase in coarse problem size due to irregular interfaces. We also plan to investigate the effect of increasing overlap size and jumping conductivity coefficients on the EMI-GDSW performance.

Acknowledgements The authors acknowledge the CINECA projects DON2CARD and OPENsCMP, the INDAM-GNCS institution and the European High-Performance Computing Joint Undertaking (JU) EuroHPC under grants agreement No 955495 (MICROCARD) and No 101172576 (MICROCARD-2). All authors have been supported by MUR grants (PRIN P2022B38NR.001 and PRIN P2022B38NR.002), funded by European Union - Next Generation EU.

References

1. Balay, S., et al.: Petsc/tao users manual. Tech. Rep. ANL-21/39 - Revision 3.20, Argonne National Laboratory (2023)
2. Centofanti, E., Huynh, N.M.M., Pavarino, L.F., Scacchi, S.: Parallel algebraic multigrid solvers for composite discontinuous galerkin discretization of the cardiac emi model in heterogeneous media. *Comput. Methods Appl. Mech. Eng.* **442**, 118001 (2025)
3. Centofanti, E., Scacchi, S.: A comparison of algebraic multigrid bidomain solvers on hybrid cpu-gpu architectures. *Comput. Methods Appl. Mech. Eng.* **423**, 116875 (2024)
4. Colli Franzone, P., Pavarino, L.F., Scacchi, S.: *Mathematical Cardiac Electrophysiology*. Springer (2014)
5. Dohrmann, C.R., Klawonn, A., Widlund, O.B.: Domain decomposition for less regular subdomains: Overlapping schwarz in two dimensions. *SIAM J. Numer. Anal.* **46**(4), 2153–2168

- (2008)
6. Dohrmann, C.R., Widlund, O.B.: An overlapping Schwarz algorithm for almost incompressible elasticity. *SIAM J. Numer. Anal.* **47**(4), 2897–2923 (2009)
 7. Goebel, F., Huynh, N.M.M., Chegini, F., Pavarino, L., Weiser, M., Scacchi, S., Anzt, H.: A BDDC Preconditioner for the Cardiac EMI Model in three Dimensions (2025). ArXiv preprint arXiv:2502.07722
 8. Huynh, N.M.M., Chegini, F., Pavarino, L.F., Weiser, M., Scacchi, S.: Convergence analysis of BDDC preconditioners for composite DG discretizations of the cardiac cell-by-cell model. *SIAM J. Sci. Comput.* **45**(6), A2836–A2857 (2023)
 9. Huynh, N.M.M., Pavarino, L.F., Scacchi, S.: GDSW preconditioners for composite discontinuous Galerkin discretizations of multicompartment reaction-diffusion problems. *Comput. Methods Appl. Math. Eng.* **433**, 117501 (2025)
 10. Jaeger, K.H., Trotter, J.D., Cai, X., Arevalo, H., Tveito, A.: Evaluating computational efforts and physiological resolution of mathematical models of cardiac tissue. *Scientific Reports* **14**, 16954 (2024)
 11. Potse, M., Saillard, E., Barthou, D., Coudière, Y.: Feasibility of whole-heart electrophysiological models with near-cellular resolution. In: *Computing in Cardiology 2020*, pp. 1–4. IEEE (2020)
 12. Ranjan, R., Chiamvimonvat, N., Thakor, N.V., Tomaselli, G.F., Marban, E.: Mechanism of anode break stimulation in the heart. *Biophys. J.* **74**(4), 1850–1863 (1998)
 13. Steyer, J.F., Chegini, F., Stry, T., Potse, M., Weiser, M., Loewe, A.: Electrograms in a cardiac cell-by-cell model. In: *Proceedings of the Workshop Biosignal 24*. Goettingen, Germany (2024)
 14. Tveito, A., Jaeger, K.H., Kuchta, M., Mardal, K., Rognes, M.E.: A cell-based framework for numerical modeling of electrical conduction in cardiac tissue. *Front. Phys.* **5**, 48 (2017)
 15. Tveito, A., Mardal, K., Rognes, M.E.: *Modeling excitable tissue: The EMI framework*. Springer Nature (2021)
 16. Veneroni, M.: Reaction–diffusion systems for the microscopic cellular model of the cardiac electric field. *Math. Methods Appl. Sci.* **29**(14), 1631–1661 (2006)